Accepted Manuscript

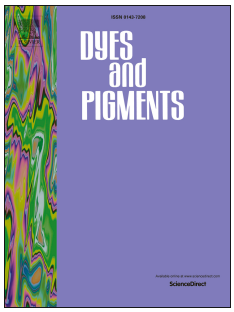

Design, synthesis and fluorescence analysis of potential fluorescent markers based on cardanol and glycerol

Felipe C. Braga, Avvari N. Prasad, Roberto da Silva Gomes, Valter A. do Nascimento, Samuel L. Oliveira, Anderson R.L. Caires, Dênis P. de Lima, Adilson Beatriz

PII: S0143-7208(16)31181-0

DOI: 10.1016/j.dyepig.2017.02.032

Reference: DYPI 5810

To appear in: *Dyes and Pigments*

Received Date: 12 November 2016

Revised Date: 3 February 2017

Accepted Date: 16 February 2017

Please cite this article as: Braga FC, Prasad AN, da Silva Gomes R, do Nascimento VA, Oliveira SL, Caires ARL, de Lima DP, Beatriz A, Design, synthesis and fluorescence analysis of potential fluorescent markers based on cardanol and glycerol, *Dyes and Pigments* (2017), doi: 10.1016/j.dyepig.2017.02.032.

Design, synthesis and fluorescence analysis of potential fluorescent markers based on cardanol and glycerol

Felipe C. Braga, Avvari N. Prasad, Roberto da Silva Gomes, Valter A. do Nascimento, Samuel L. Oliveira, Anderson R. L. Caires, Dênis P. de Lima, and Adilson Beatriz

We provide an alternative to use cardanol and glycerol as building blocks to produce six structurally, amphiphilic molecules. The *meta*-triazolaniline (**1b**) presented a high fluorescent signal at low concentration (4 ppm), revealing to be the best candidate for a fuel marker.

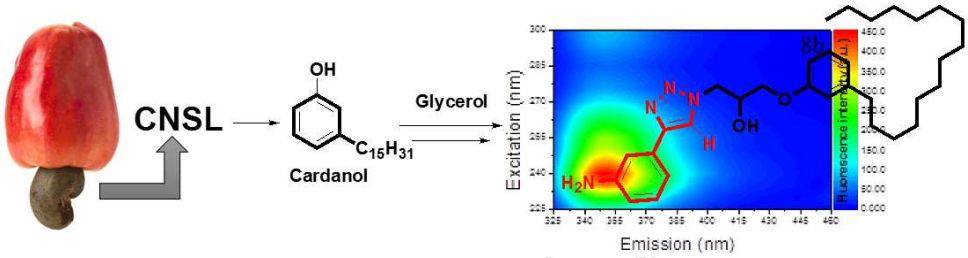

Design, synthesis and fluorescence analysis of potential fluorescent markers based on cardanol and glycerol

Felipe C. Braga,[a†] Avvari N. Prasad,[a†] Roberto da Silva Gomes,[b] Valter A. do Nascimento,[c] Samuel L. Oliveira,[d] Anderson R. L. Caires,*[d] Dênis P. de Lima[a], and Adilson Beatriz*[a]

[a]Instituto de Química, Universidade Federal de Mato Grosso do Sul. Av. Senador Filinto Müller, 1555, CEP: 79074-460, Campo Grande, MS, Brazil

[b]Faculdade de Ciência Exatas e Tecnologia, Universidade Federal da Grande Dourados, Itahum, km 12 – Cidade Universitária, 79804-970, Dourados, MS, Brazil

[c]Grupo de Espectroscopia e Bioinformática Aplicados a Biodiversidade e a Saúde, Faculdade de Medicina, CP 549, 79070-900 Campo Grande, MS, Brazil.

[d]Grupo de Óptica e Fotônica, Instituto de Física, Universidade Federal de Mato Grosso do Sul, CP 549, 79070-900 Campo Grande, MS, Brazil.

*Corresponding authors:

Adilson Beatriz, e-mail: adilson.beatriz@ufms.br

Anderson R. L. Caires, e-mail: anderson.caires@ufms.br

† These authors contribute equally to this work.

Abstract

We report the synthesis and fluorescent properties of 1,4-disubstituted-1,2,3-triazoles (**1a-c**) based on pollutant wastes and by-products from the cashew and biodiesel industries as a design for fluorescent markers. The triazoles were synthesized in four steps; catalytic hydrogenation of cardanol, reaction with epichlorohydrin, azide substitution and/or epoxide opening and, Cu catalyzed click-chemistry of the azide with the ethynylanilines (**6a-c**). This procedure is a potential alternative to make fluorescent markers since it affords the intermediates in high yields, enabling one to produce the products in good quantities. Moreover, triazolazobenzenes (**8a-c**) were prepared by azo coupling of the trizoles (**1a-c**) with phenol to give a new option of dyes. Evaluation of the fluorescent properties of the achieved compounds showed that all triazole derivatives displayed good fluorescence emissions in the range of 325 to 400 nm, with a maximum of fluorescence intensity at around 350 nm when excited between 225 and 300 nm; besides, the *para*-triazolaniline exhibited a dual fluorescence emission, presenting an additional emission band in the blue range (400-500 nm).

Introduction

Organic compounds endowed with special photophysical properties, usually dyes, are important for the development of many products such as photodynamic therapy photosensitizers[1], biomarkers[2], components of solar cells[3], chemical catalysts[4], fuel industry markers[5] and other technological products[6]. Fuel fluorescent markers have been drawing the attention of many scientists since they can be applied as "silent" markers because they are invisible in ambient light, but can be easily detected by their fluorescence[7], offering many vantages in comparison with colored products. However, there are certainly unresolved issues to achieve a perfect fluorescent marker,[8] making the research in this field very promising, especially if one selects the biomass as a source of raw material to prepare these compounds.

The Cashew Nut Shell Liquid (CNSL) is one of the low cost, bio based, and naturally occurring resources of non-isoprenoid phenolic lipids consisting mainly of cardanol.[9] CNSL is produced in the food industry during one of the steps to get the cashew almond, by solvent extraction of the cashew nut. It consists of anacardic acid (46-65%), cardanol (10-22%), cardol (15-31%), traces of 2-methyl-cardol and others (0-2%), with their percentage varying depending on the extraction process (Figure 1).[10-12] In the industry the nut is heated up to 300 °C, during this process the CNSL's main component (anacardic acid) is converted to cardanol through decarboxylation, increasing its percentage to 68-74%. CNSL represents nearly 25% of the nut weight and its production worldwide is estimated to about 300,000 tons per year which leads it to be a powerful phenolic pollutant.[13] On the other hand, cardanol can be considered as a building block for chemical synthesis and it adds value to the CNSL generated in the cashew productive chain.[13-15] Some successful examples of amphiphilic molecular hybrid systems prepared from cardanol, such as phthalocyanines[16] and porphyrins,[7,17,18] prompted the search for new applications such as herein described as a main topic.

[Figure 1 near here]

Currently, another important industrial residue is glycerol. Its use in the synthesis of higher value chemicals has been highlighted in the green chemistry area for the last few years. The exponential growth of biodiesel production, in which glycerol is generated as by-product raised an enormous concern about its environmental impact. In fact, the glycerol disposal is a major issue in the mass production of biodiesel and it is desirable to find

alternatives for the consumption of extra volume of crude glycerol.[19] Thus, glycerol has been used as a versatile primary chemical building block to produce a great variety of commercially valuable compounds.[20-24]

Taking into account the characteristics of the compounds previously mentioned, we aim to combine their properties into single compounds with unique potentials. Herein we report the design and synthesis of fluorescent amphiphilic molecules to function as potential fluorescent markers, bearing a fluorophore and a hydrophobic group. The fluorophore consists in an aniline coupled with a 1,2,3-triazole to complete the chromophoric system that guarantees a fluorescent emission (Figure 2). 1,4-disubstituted-1,2,3-triazoles are simply prepared by ‘‘Click chemistry’’, and they have been motifs in medicinal chemistry, used as molecular chemical sensors and important linkers of conjugated systems.[25,26] Besides it is a simple reaction that involves only non-toxic reactants and green conditions. In the meantime, the hydrophobic group (cardanol moiety) is sufficiently nonpolar to make it soluble in biodiesel, for example.

[Figure 2 near here]

The target compounds were prepared from glycerol and cardanol. The photophysical properties were determined by UV-Vis absorption and steady-state fluorescence analysis. Characterization of the compounds was carried out by NMR (^{1}H and ^{13}C), IR spectroscopy, and high-resolution mass spectrometry.

Results and discussion

A retrosynthesis analysis for the fluorescent amphipathic compounds is displayed in Scheme 1. The 1,4-disubstituted-1,2,3-triazoles **1a-c** can be generated via “Click chemistry”[27] starting from azide **7** and the ethynylanilines **6a-c**. The linkage between saturated cardanol (**2**) and glycerol (**3**) can be easily made through a glycerol derivative epichlorohydrin (**4**), which is easily obtained from glycerol.[28]

[Scheme 1 near here]

To start the synthetic route, cardanol was isolated from CNSL, which was provided from a local industry. The CNSL was initially filtered to remove solid impurities, and then distilled under vacuum. The liquid obtained through distillation is a mixture of cardanol with different number of double bonds in the side chain, though the main compound present is the monounsaturated side-chain phenol.

This mixture of cardanols was then hydrogenated with Pd/C 5%. The reaction is fast and the catalyst can be filtered off and used again after proper treatment. The product is purified by crystallization in cold solvent and affords white pure powder (**2**) in 94% yield.

For the next step, cardanol (**2**), epichlorohydrin (**4**) and DMAP (4-dimethylaminopyridine) were heated under reflux to give a mixture of products **5a** and **5b** (Scheme 2). This methodology was improved in comparison with a previous one that used pyridine. It seems that the pyridine drove the reaction to an undesired path forming a side product. The use of a hindered catalyst proved to be better, therefore DMAP was selected to increase the yield from 40% to about 90% overall. Compounds **5a** and **5b** were achieved with ~54% and ~36% yield, respectively, and were substrates for the following steps.

[Scheme 2 near here]

Although two different compounds are inevitably generated from this reaction, both products can be used to generate the azide compound **7** in excellent yields. Thus, we carried out two pathways as an atom economic procedure using compounds **5a** and **5b** to give the desired product.

The generality of epoxide opening was tested using a range of solvents to afford reasonable to excellent yields (Table 1). Poly(ethylene glycol) (PEG- 400) was found to be the most appropriate solvent system to achieve compound **7** with high yield (Table 1, Entry 6). Recently, PEG has attracted interest as a solvent due to its distinctive properties including inexpensive, easy degradability and, low-toxicity, thus, improving green conditions.[29-33] Although compound **7** can be distinguished from its precursors by NMR analysis, **5b** and **7** present similar spectra but they differ in the IR spectra, which shows a characteristic stretching band for the N_3 group at 2098 cm^{-1}.[34]

[Table 1 near here]

Subsequently, compound **7** was subjected to “click chemistry” through CuAAC cycloaddition of azide and terminal alkynes to attain the corresponding triazoles.[35,36] To

determine the best catalytic system for this transformation, we optimized typical reaction parameters such as various Cu catalysts, solvents and, temperature, as illustrated in Table 2. Among all catalysts, metallic copper powder in presence of water:acetone (2:1) exhibited great catalytic activity towards the desired triazole under mild conditions (Table 2, Entry 9). Thus, triazoanilines **1a-c** were obtained by treatment of compound **7** with alkynes **6a-c** (Scheme 3).

[Scheme 3 near here]

[Table 2 near here]

In spite of existing few fluorescent azobenzenes,[37] some derivatives can show high fluorescence quantum yields, mainly those that are able to make interaction between the nitrogen atom and electron acceptors.[38] Besides, azo dyes are very important choromophores largely used in textile industry and for the preparation of many high-tech futuristic materials[3a,5a] Herein, owing to the nature of the groups in the target molecules, we have decided to add an addition step to the route and react the triazoles **1a-c** into the corresponding azobenzenes **8a-c**, and study their photophysical properties. Therefore, compounds **1a-c** were submitted to azo coupling reaction with sodium nitrite at 0 ^{o}C followed by treatment with a phenoxide solution to give **8a-c** (Scheme 4). All three compounds are *E* isomers. The conversion to the less thermodynamically stable *Z* isomer may be achieved upon UV irradiation.[39]

[Scheme 4 near here]

Photophysical Studies

UV-Vis spectra of triazolanilines (**1a-c**) are showed in Figure 3. The results showed that the maximum absorption wavelength had correlation with the NH_2 substituent position on benzene ring (*ortho*, *meta* or *para*). An absorption centred at 206 nm (*range **a***) was observed for all compounds. In contrast, a well-defined maximum absorption at 230 nm (*range **b***) was observed for compounds **1a-b** and a small shoulder for compound **1c**. In addition, an absorption shoulder at around 254 nm (*range **c***) was observed for compounds **1a-b** while only compound **1c** exhibited an intense absorption band centred at 280 nm (*range **c***). Moreover, all compounds presented a small absorption band over 290-350 nm range (*range **d***), centred at 308 nm for compounds **1b-c** and red-shifted to 320 nm for compound **1a.** To identify the nature of these bands, we performed ground state calculations using the Austin Model 1 (AM1) semi-empirical method in Hyperchem 7.5

Software. The AM1 is a semi-empirical method able to perform quantum calculation of molecular electronic structure in computational modelling.[40] The structures were then geometrically optimized using the Polak-Ribiere method. After geometric optimization, single-point calculations were performed using ZINDO/S parameters with the configuration interaction (CI) method set to "Singly Excited". The ZINDO/S method has proven to be extremely accurate in calculating electronic transitions energies and intensities of both absorption an emission.[41,42] In accordance to the experimental observations, the theoretical results showed that the electronic transitions were NH_2 substituent position dependent. The absorption at around 205 nm (*range* ***a***) was obtained for all compounds while strong absorptions in the *range* ***b*** (210-250nm) were observed for compounds **1a** and **1b** (Table 3). Finally, as observed in the experimental result, a maximum absorption band at around 284nm was determined only for compound **1c.** All electronic transitions in the UV-Vis range, with its respective wavelength and oscillator strength, obtained by AM1 semi-empirical method are showed in Table S1 (see Supplementary material). AM1 calculations also revealed that the electrons located at around the benzene ring with NH_2 as substituent as well as in the ring containing the N atoms have played key role in the electronic transitions (see the electronic densities for the HOMO and LUMO states in Fig. S1 - S3 (see Supplementary material). In fact, as expected, the substituent NH_2 behaved as a donor group while the triazole ring as an acceptor group. Additionally, it is well established that the absorption bands at around 210 and 254 nm are attributed to the benzene ring as well as the absorption at 235 and 285 nm are assigned to the aniline molecule (a benzene ring containing a NH_2 as substituent) due to the intramolecular charge transfer (ICT) from de donor group (NH_2) to the benzene ring as demonstrated by Kimura et al. by analysing the vacuum UV absorption spectra of aniline and its derivatives.[43,44] Finally, it is worth to point out that absorption bands over 300 nm with significant oscillator strength were not detected by the theoretical calculation, probably due to the fact that the AM1 calculation was performed assuming the absence of solvent (in vacuum).

[Figure 3 near here]

[Table 3 near here]

The fluorescence results revealed that emission intensity was strongly dependent of substituent position in which the compound **1b** (*meta*-aniline) presented higher fluorescence intensity as shown in Fig. 4. Despite the difference in the fluorescence intensity, the inset in Fig. 4 shows that all compounds (**1a-c**) presented an emission band in the UV range (between 300 and 400 nm) induced by the Locally Excited (LE) state. However, in addition to the emission from LE state, *para*-aniline

1c presented an additional emission band in the blue range (between 400 and 500 nm) as a result of an extra relaxation channel, perhaps originated from the emergence of a Twisted Intramolecular Charge Transfer (TICT) state due to an intramolecular charge transfer accompanied by an internal rotation within the fluorophore. It is well known that molecules containing aniline group can present the observed dual fluorescence behaviour due to emission from the LE state and an extra emission band corresponding to transition from the TICT state at higher wavelengths.[44] The dual fluorescence behaviour of **1c**, with a blue emission band, can be also visualized in the excitation-emission contour map presented in Fig. 5. These data show that **1a-c** exhibited fluorescence in the 325 to 400 nm range, with a maximum at around 350 nm, when excited between 225 and 300 nm while only **1c** presented the blue emission (between 400 and 460 nm) when excited in the 225-300 nm range. The excitation-emission map is totally in accordance with the determined absorbance as the maximum emission was observed for an excitation at 240 nm for **1a-b** and 270 nm for **1c**. Finally, it is important to point out that the contour maps were built using different fluorescence intensity scales for a better visualization of the emissions, consequently, the excitation and emission maps also stress that **1b** presented higher fluorescence intensity.

To investigate the difference observed in the intensities, the relative fluorescence quantum yields (Φ_F) were determined by analysing the fluorescence and absorption spectra of **1a-c**. The analyses were performed by following the steps presented in details in a recent paper published by our group[45] where the relative fluorescence quantum yield ratio can be determined by Eq. 1:

$$\frac{\Phi_{F1}}{\Phi_{F2}} = \frac{A_{F1}.I_{A2}}{A_{F2}.I_{A1}}$$

Eq. 1

Where I_A is the absorption intensity (absorbance) at a wavelength (λ_E) and A_F is the area under the emission curve, calculated by $\int I_F(\lambda_E, \lambda_F) d\lambda_F$, produced by an excitation at λ_E. As presented in Table 4, the results revealed that Φ_F of compound **1b** was 9.35 and 6.32 higher than Φ_F of compound **1a** and **1c**, respectively. The calculations were carried out considering the absorbance value and excitation wavelength at 265 nm and the emission in the 310-510 range, using the values obtained from excitation-emission spectra presented in Fig. 5.

[Figure 4 near here]

[Table 4 near here]

[Figure 5 near here]

Furthermore, when compounds **1a-c** were under UV light (254 nm) they all changed their colour to green (see Supplementary material, Fig. S7); that is a good indication of their potential application as markers, since a simple test such as using incident UV light is enough to identify their presence.[46]

The optical features of **8a-c** were also determined by measuring their absorbance and fluorescence spectra. The UV-Vis analysis showed that the azocompounds **8a-c** presented different optical characteristics as a function of diazenylphenol moiety position (Fig. 6). The results indicated that compounds **8a-b** presented three absorption bands at around 210, 248, and 345 nm in the absorption ranges ***a***, ***b*** and ***c***, respectively. However, compound **8b** showed higher absorbance than compounds **8a**; for instance, it presented a maximum absorption value in the range ***c*** 18 times higher than compound **8b**. The electronic transitions responsible for these absorptions may be related to the electrons located at around the diazophenol group since the 248 and 345 nm have been assigned to the nitrophenol and azobenzene molecules.[47,48] In contrast, the compound **8c** absorbed significantly at 210 nm (range ***a***), showing only the benzene absorption feature as the diazophenol bands (at 248 and 345 nm) were suppressed. Although a decrease of absorption, as observed for **8c** when compared with **8a-b**, may be related to a possible difference in the rotational restriction around N=N bond. Further investigations are necessary since no conclusive answer is available from the obtained results. For the diazenylphenol compounds the AM1 semi-empirical method calculations were also performed to obtain the electronic transitions and the electronic densities for the HOMO and LUMO states. The main electronic transitions obtained theoretically are showed in Table 5. As experimentally observed, the theoretical results also revealed that the electronic transitions were diazophenol substituent position dependent. Furthermore, the electronic density of the HOMO and LUMO states indicated that the electrons from diazophenol group are involved in the main electronic transitions (see Supplementary material, Fig. S4 – S6).

[Table 5 near here]

[Figure 6 near here]

Differently from triazolanilines **1a-c**, the fluorescence measurements revealed that **8a-c** did not exhibit fluorescence signal when diluted at 4 ppm. In fact, only **8a** and **8c** presented low emission intensity in the UV range even at high concentration (at 100 ppm), with a maximum at around 350 nm under excitation between 225 and 300 nm (see Supplementary material, Fig. S8). These low fluorescence quantum yields of azobenzenes **8a-c** when compared with the correspondent triazolanilines (**1a-c**) can be explained for the fact that **8a-c** have an additional ring (phenol),

permitting additional non-radiative relaxation due to the decrease of molecular rigidity.[49] Besides, it is known that azobenzenes experiment efficient isomerization under photoexcitation, leading to low fluorescence emission.[38]

Simultaneous thermal analysis (TG/DSC) was used to study the thermal behavior of compounds **1a-c**. Endothermic peaks are observed at 83.2 °C, 89.2 ^{o}C and 122.9 ^{o}C corresponding to melting points of compounds **1a**, **1b** and **1c**, respectively. Exothermic peaks are observed at around 350 °C for all compounds, corresponding to its oxidations. The thermal stabilities are 266 ^{o}C for **1a**, 293 ^{o}C for **1b** and 223 ^{o}C for **1c (see** supplementary material, Figure S9).

Experimental Part

General remarks

All reactions were carried out in clean glassware with magnetic stirring with the exception of the catalytic hydrogenation that was carried out in a Parr Hydrogenation apparatus. Chromatographic purification was performed on silica gel (Merck 100-200 mesh) and analytical thin layer chromatography (TLC) on silica gel 60-F_{254}, which was detected by fluorescence. ^{1}H NMR (300 MHz) and ^{13}C NMR (75 MHz) spectra were measured with a Bruker Avance DPX-300 spectrometer with $CDCl_3$ and DMSO-D_6 as solvents and recorded in ppm relative to internal tetramethylsilane standard. The ^{1}H NMR spectra are reported as follows: δ/ppm (multiplicity, coupling constant *J*/Hz, number of protons). Multiplicity is abbreviated as follows: s = singlet, d = doublet, doublet of doublets (dd), t = triplet, m = multiplet. Coupling constants (*J*) are quoted in Hertz and recorded to the nearest 0.1 Hz. High-resolution mass spectroscopy (HRMS) was performed on a UFLC Shimadzu LC-20AD apparatus, with and IES-Q-QTOF-microTOF III detector (Bruker Daltonics) in chemical ionization positive ion mode (m/z 120-1200). The samples were prepared with 0.1 g/mL (methanol/ water 7:3) and injected 1 μL, using elution gradient water (phase A) and acetonitrile (phase B), both with acetic acid 1%, isocratic method 50% and the running time of 3 minutes. The infrared spectra were recorded on a FT-IR spectrometer and reported as wavenumbers (cm^{-1}). The melting point of the compounds was determined using a Quimis® 0340S23 melting point apparatus.

UV-Vis absorption measurements were performed using an absorption spectrophotometer (Cary 50), containing a pulsed xenon lamp, a 0.25 m Czerny–Turner monochromator and a Si diode detector. The UV-Vis spectra were measured in the 200-800 nm range by analysing diluted samples in dichloromethane (CH_2Cl_2) at 4 ppm. Fluorescence measurements were

collected by a spectrofluorimeter (Cary Eclipse) using a pulsed xenon lamp (80 Hz), with peak power equivalent to 75 kW, as excitation source and a photomultiplier tube (R928) as a fluorescence detector. The excitation and emission wavelengths were selected by using two Czerny–Turner monochromators. The emission-excitation counter maps were determined by collecting the emission between 220 and 520 nm when exciting in the 220-420 nm range. For all spectroscopic analysis, the samples were diluted in dichloromethane (CH_2Cl_2) and the measurements were performed at room temperature using a quartz cuvette with four polished faces and 1 cm optical path length. The fluorescence measurements were carried out using the right-angle geometry (i.e. the fluorescence was collected at a 90^0 angle in respect to the excitation light).

Simultaneous TG–DSC curves were obtained with a thermal analysis system, model STA 449 F3 Jupiter® and experimental data were obtained through Proteus® Software. It was employed alumina crucibles with sample masses near to 5.0 mg on purge gas flow (air) of 50 mL min^{-1} and heating rate optimized for 20 ^oC min^{-1}.

Synthesis

Extraction procedure of cardanol mixture from CNSL. Vacuum distillation was used in this extraction, where 53.25 g of CNSL was heated to about 300^{o}C for 4 h, under reduced pressure in a short Path apparatus to give a 39.41 g (74%) of a cardanol mixture rich in monounsaturated cardanol.

Cardanol mixture. (74% yield). Yellow oil. R_f= 0.33 (Hexane/EtOAc, 9:1); ^{1}H NMR (300.13 MHz, $CDCl_3$) δ 7.13 (t, ^{3}J(H,H) = 7.5 Hz, 1H; Ar-H), 6.75 (d, ^{3}J(H,H) = 7.7 Hz, 1H; Ar-H), 6.66 (s, 1H; Ar-H), 6.63 (d, 1H; Ar-H), 5.35 (m, 2H; CH=CH), 2.78 (m, 1H;CH), 2.54 (t, ^{3}J(H,H) = 7.7 Hz, 2H; Ar-CH_2C), 2.02 (m, 3H; CH_3), 1.58 (m, 2H; CH_2), 1.30 (m, 14H;CH_2), 0.88 (m, 3H; CH_3); ^{13}C NMR (75.48 MHz, $CDCl_3$) δ 155.45 (ArC-OH), 144.94 (ArC), 130.03, 129.91 (2x =CH), 129.45, 120.94, 115.45, 112.63 (4x ArCH), 35.90, 31.36, 29.80, 29.30, 27.27, 22.74 (13xCH_2), 14.18 (CH_3).

Typical procedure for the preparation of compound 2. The catalytic hydrogenation was carried out in a Parr Hydrogenation apparatus. Pd/C (250 mg) was added to a solution of cardanol mixture (5 g) in ethyl acetate (30 mL) and submitted to 60 Psi of hydrogen gas. After 5h, the solution was filtered, to separate the catalyst, then the solvent was evaporated and the solid was recrystallized with cold hexane (0^{o}C) to give 4.70 g of compound **2** (93% yield).

3-Pentadecylphenol (2). (76% yield). White powder. Mp: 40-43 ^{o}C. R_f= 0.33 (Hexane/EtOAc,

9:1); ^{1}H NMR (300.13 MHz, $CDCl_3$) δ 7.12 (t, ^{3}J(H,H) = 6.0 Hz, 1H; Ar-H), 6.73 (d, ^{3}J(H,H) = 6.0 Hz, 1H; Ar-H), 6.66 (s, 1H; Ar-H), 6.63 (m, 1H; Ar-H), 2.53 (t, ^{3}J(H,H) = 9.0 Hz, 2H; Ar-CH_2), 1.57 (m, 2H; CH_2), 1.24 (m, 24H; CH_2), 0.87 (m, 3H; CH_3); ^{13}C NMR (75.48 MHz, $CDCl_3$) δ 155.37 (ArC-OH), 144.97 (ArC), 129.35, 120.97, 115.31, 112.47 (4x ArC-H), 35.82, 31.91, 31.28, 29.68, 29.59, 29.32, 22.69 (14x CH_2), 14.10 (CH_3).

Synthesis and isolation of 5a and 5b. To a solution of compound **2** (2.0 g, 6.58 mmol) in epichlorohydrin (8.5 mL, 0.82 mol), catalytic quantity of DMAP was added (36 mg, 0.29 mmol) and the mixture was kept under reflux for 4h. Then, the solution was washed with water and dried over anhydrous sodium sulfate. Filtration followed by evaporation of the solvent led to the mixture of **5a** and **5b** that were separated by silica gel chromatography to give 54% and 36% yields, respectively.

2-[(3-pentadecylphenoxy)methyl]oxirane (5a). (54% yield). White solid. Mp: 40-43 °C. R_f= 0.63 (Hexane/EtOAc, 9:1); 1H NMR (300.13 MHz, $CDCl_3$) δ 7.16 (t, 3J(H,H) = 7.71 Hz, 1H; Ar-H), 6.77 (d, 3J(H,H) = 7.67 Hz, 1H; Ar-H), 6.73 (s, 1H; Ar-H), 6.71 (m, 1H; Ar-H), 4.17 (dd, 3J(H,H) = 11.04 Hz, 2J(H,H) = 3.29 Hz, 1H; O-CH_2), 3.95 (dd, 3J(H,H) = 10.96 Hz, 2J(H,H) = 5.55 Hz, 1H; O-CH_2), 3.34 (m, CH-O-), 2.88 (t, 3J(H,H) = 4.49 Hz, 1H; epoxide-CH_2), 2.74 (dd, 3J(H,H) = 4.90 Hz, 2J(H,H) = 2.63 Hz, 1H; epoxide-CH_2), 2.55 (t, 3J(H,H) = 7.45 Hz, 2H; CH_2), 1.55 (m, 2H; CH_2), 1.23 (m, 24H; CH_2), 0.86 (t,3J(H,H) = 6.39 Hz, 3H; CH_3); ^{13}C NMR (75.48 MHz, $CDCl_3$) δ 158.54 (ArC-O), 144.67 (ArC-), 129.21, 121.44, 114.96, 111.47 (4x ArCH), 68.61 (ArO-CH_2), 50.21 (CH-epoxide), 44.68 (epoxide-CH_2), 36.07, 32.04, 31.46, 29.80, 29.71, 29.63, 29.48, 29.43, 22.79 (14x CH_2), 14.20 (CH_3).

1-chloro-3-(3-pentadecylphenoxy)propano-2-ol (5b). (36% yield). White solid. R_f= 0.33 (Hexane/EtOAc, 9:1); ^{1}H NMR (300.13 MHz, $CDCl_3$) δ 7.18 (t, ^{3}J(H,H) = 7.64 Hz, 1H; Ar-H), 6.79 (d, ^{3}J(H,H) = 6.79 Hz, 1H; Ar-H), 6.73 (s, 1H; Ar-H), 6.70 (m, 1H; Ar-H), 4.19 (m, 1H; HO-CH), 4.02 (m, 2H; O-CH_2) 3.74 (m, 2H; CH_2-Cl), 2.55 (t, ^{3}J(H,H) = 7.75 Hz, 2H; CH_2), 1.58 (m, 2H; CH_2), 1.24 (m, 24H, CH_2), 0.86 (t,^{3}J(H,H) = 6.39 Hz, 3H; CH_3); ^{13}C NMR (75.48 MHz, $CDCl_3$) δ 158.18 (ArC-O), 144.88 (ArC), 129.29, 121.65, 114.76, 111.45 (4x ArCH), 69.92 (CH-OH), 68.32 (O-CH_2), 45.98 (CH_2-Cl), 36.00, 31.93, 31.40, 29.68, 29.59, 29.51, 29.36, 29.35, 22.70 (14x CH_2), 14.13 (CH_3).

Synthesis of compound 7 pathway 5a to 7. Sodium azide (140 mg, 2.15 mmol) was added to a solution of the epoxide **5a** (520 mg, 1.44 mmol) in PEG 400 (4.40 mL). The solution was stirred at 60°C for 4 h and then diluted with ethyl acetate (10 mL). The solution was washed with brine (3x 5

mL) and the organic layer was dried with anhydrous sodium sulfate. Filtration followed by evaporation of the solvent led to the crude product that was purified by silica gel chromatography to yield the correspondent azide **7** (506 mg, 1.25 mmol, 87%).

Synthesis of compound 7 pathway 5b to 7. A mixture of compound **5b** (765 mg, 1.93 mmol) and Sodium azide (250 mg, 3.85 mmol) and 3 mL of DMSO was stirred at 80°C for 6h. Then the reaction mixture was poured into water (10 mL), extracted with hexane - diethyl ethyl (1:1) mixture (2x 10 mL). The extracts were washed with brine (10 mL), dried over anhydrous sodium sulphate and evaporated. The residue was dried under vacuum at room temperature to afford a colourless oil (**7**). (757 mg, 1.87 mmol, 97%).

1-(3-pentadecylphenoxy)-3-(2-triaz-1-en-2-yn-1-yl)propan-2-ol (7). (87% yield). Yellow oil. R_f= 0.35 (Hexane/EtOAc, 9:1); IR (film) ν_{max} 3409, 2923, 2854, 2102, 1593, 1446, 1269, 1099, 1053, 945, 875 cm^{-1}; ^{1}H NMR (300.13 MHz, $CDCl_3$) δ 7.17 (t, ^{3}J(H,H) = 7.67 Hz, 1H; Ar-H), 6.79 (d, ^{2}J(H,H) = 7.38 Hz, 1H; Ar-H), 6.74 (s, 1H; Ar-H), 6.70 (m, 1H; Ar-H), 4.14 (m, 1H; CH-OH), 3.98 (d, ^{3}J(H,H) = 5.04 Hz, 2H; O-CH_2), 3.49 (m, 2H; CH_2-N_3), 2.57 (t, ^{3}J(H,H) = 7.56 Hz, 1H; Ar-CH_2), 1.60 (m, 2H; CH_2), 1.27 (m, 24H; CH_2), 0.89 (m, 3H; CH_3); ^{13}C NMR (75.48 MHz, $CDCl_3$) δ 158.30 (ArC-O), 144.82 (ArC-), 129.26, 121.59, 114.80, 111.50 (4x ArC-H), 69.34 (CH-OH), 69.00 (O-CH_2), 53.50 (CH_2-N_3), 36.03 (Ar-CH_2), 31.96, 31.41, 29.72, 29.64, 29.55, 29.39, 22.71 (13x CH_2), 14.13 (CH_3).

General procedure for the preparation of 1a-c. Example for **1a**: To a 10 mL round bottom flask, 2-ethynylaniline (137 mg, 1.17 mmol) and powdered copper metal (20 mg, 0.31 mmol) was added to a solution of compound **7** (314 mg, 0.78 mmol) in 2.5 mL of water:acetone (2:1). The mixture was stirred for 12h. After completion of the reaction, ethyl acetate was added to the solution, washed with water and, the organic layer was dried and evaporated. The crude residue was purified by silica gel chromatography to yield compound **1a** (272 mg, 0.52mmol, 67%).

1-[4-(2-aminolphenyl)-1H-1,2,3-triazol-1-yl]-3-(3-pentadecylphenoxy)propan-2-ol (1a). (54% yield). Brown solid. Mp: 80-85 ^{o}C. R_f= 0.15 (hexane/EtOAc, 8:2); ^{1}H NMR (300.13 MHz, $CDCl_3$) δ 8.43 (s, 1H; NCH=CNAr), 7.41 (d, ^{3}J(H,H) = 7.38 Hz, 1H; Ar-H), 7.13 (t, ^{3}J(H,H) = 7.89 Hz, 1H; Ar-H), 6.98 (t, ^{3}J(H,H) = 7.27 Hz, 1H; Ar-H), 6.72 (m, 4H; Ar-H), 6.54 (t, ^{3}J(H,H) = 7.13 Hz, 1H; Ar-H), 6.15 (s, 2H; NH_2), 5.58 (d, ^{3}J(H,H) = 5.19 Hz, 1H; Ar-H), 4.60 (dd, ^{2}J(H,H) = 13.67 Hz, ^{3}J(H,H) = 2.70 Hz, 1H; O-CH_2), 4.43 (dd, ^{2}J(H,H) = 13.30 Hz, ^{3}J(H,H) = 7.52 Hz, 1H; O-CH_2), 5.25 (m, 1H; CH-OH), 3.91 (m, 2H; CH_2-N), 2.47 (m, 2H; Ar-CH_2), 1.49 (m, 2H; CH_2), 1.18 (m, 24H; CH_2), 0.80 (m, 3H, CH_3); ^{13}C NMR (75.48 MHz, $CDCl_3$) δ 158.83, 147.53, 146.06, 144.42 (4x ArC), 129.62, 128.75, 127.95, 122.65, 121.23 (5x ArC-H), 116.38 (Ar-C=), 116.20, 115.05 (2x ArC-H), 113.29 (CH=), 112.03 (ArC-H), 69.84 (O-CH_2), 68.34 (HO-CH), 53.34 (CH_2N), 35.69

(Ar-CH_2), 31.78, 31.36, 29.54, 29.21, 22.57 (13x CH_2), 14.34 (CH_3); HRMS (ESI) m/z calcd for $C_{32}H_{49}N_4O_2$ 512.3848, found 521.3850.

1-[4-(3-aminophenyl)-1H-1,2,3-triazol-1-yl]-3-(3-pentadecylphenoxy)propano-2-ol (1b). (39% yield). Gray solid (green in solution). Mp: 90-95 ^oC. R_f= 0.21 (hexane/EtOAc, 5.5:4.5); ^1H NMR (300.13 MHz, $CDCl_3$) δ 7.7 (s, 1H; NCH=CNAr), 7.08 (t, $^3J(H,H)$ = 7.67 Hz, 1H; Ar-H), 6.99 (m, 1H; Ar-H), 6.95 (m, 2H; Ar-H), 6.71 (d, $^3J(H,H)$ = 7.23 Hz, 1H; Ar-H), 6.67 (s, 1H;Ar-H), 6.62 (d, $^3J(H,H)$ = 8.04 Hz, 1H; Ar-H), 6.49 (d, $^3J(H,H)$ = 6.94Hz, 1H; Ar-H), 4.55 (m, 1H; CH-OH), 4.37 (m, 2H; O-CH_2), 3.91 (m, 2H; CH_2-N) 2.48 (t, $^3J(H,H)$ = 7.27 Hz, 2H, Ar-CH_2) 1.52 (m, 2H, CH_2), 1.21 (m, 24H, CH_2), 0.83 (m, 3H CH_3); ^{13}C NMR (75.48 MHz, $CDCl_3$) δ 158.23, 147.42, 146.86, 144.88, 131.05 (4x ArC and 1xAr-C=), 129.74, 129.31, 121.59, 115.97, 115.02, 114.82, 112.21, 111.41 (8x ArC-H and 1x CH=), 68.91 (O-CH_2), 68.80 (HO-CH), 53.48 (CH_2N), 36.03, 31.94, 31.45, 29.72, 29.65, 29.57, 29.42, 29.38, 22.71 (14xCH_2), 14.15 (CH_3); HRMS (ESI) m/z calcd for $C_{32}H_{49}N_4O_2$ 521.3848, found 521.3850.

1-[4-(4-aminophenyl)-1H-1,2,3-triazol-1-yl]-3-(3-pentadecylphenoxy)propano-2-ol (1c). (69% yield). Yellow solid. Mp: 120-125 ^oC. R_f= 0.30 (EtOAc/ Hexane; 5.5:4.5); ^1H NMR (300.13 MHz, $CDCl_3$) δ 7.72 (s, 1H; NCH=CNAr), 7.54 (d, $^3J(H,H)$ = 8.33 Hz, 2H; Ar-H aniline), 7.17 (t, $^3J(H,H)$ = 7.45 Hz, 1H; Ar-H cardanol), 6.79 (d, $^3J(H,H)$ = 7.45 Hz, 1H; Ar-H cardanol), 6.69 (m, 4H; 2xAr-H card and 2xAr-H aniline), 4.67 (d, 1H, CH-OH), 4.50 (m, 2H; O-CH_2), 3.98 (m, 2H; CH_2-N), 2.54 (t, $^3J(H,H)$ = 7.52 Hz, 1H; Ar-CH_2), 1.57 (m, 2H; CH_2), 1.23 (m, 24H; CH_2), 0.86 (m, 3H; CH_3); ^{13}C NMR (75.48 MHz, $CDCl_3$) δ 158. 07 (ArC-O), 148.05 (ArC-C ani), 146.51 (ArC-NH_2), 144.94 (ArC-C card), 129.32 (CH card), 126.93 (2x CH ani), 121.75 (CH card), 120.86 (=C-N), 119.99 (HC= triazol), 115.22 (2x CH ani), 114.74 (CH card), 111.48 (CH card), 69.05 (CH-OH), 68.66 (O-CH_2), 52.85 (CH_2-N_3), 35.99 (Ar-CH_2), 31.91, 31.39, 29.67, 29.59, 29.51, 29.35, 22.68 (13x CH_2), 14.10 (CH_3); HRMS (ESI) m/z calcd for $C_{32}H_{49}N_4O_2$ 521.3853, found 521.3850.

General procedure for the preparation of diazenyl compounds 8a-c. Example for **8b**: Five drops of HCl 6M at 0 ^oC were added to a solution of **1b** (86 mg, 0.16 mmol) in methanol (5 mL). A solution of sodium nitrite (57 mg, 0.83 mmol) in water (1.5 ml) at 0 ^oC was added and stirred for 30 min. The temperature was kept at 0-5 ^oC throughout the reaction time. To the diazonium salt solution formed was added a cold solution of phenol (23 mg, 0.24 mmol) in NaOH 7M (2.5 mL), keeping the temperature around 0 ^oC, when TLC monitoring indicated completion of the reaction (8h). The solution was acidified with HCl 6M (until pH<9) and ethyl acetate was added (10 mL). The organic layer was washed with brine (3 x 5 mL), dried over anhydrous sodium sulphate, filtered and, the solvent evaporated under reduced pressure. The crude residue was purified by silica gel chromatography to yield **8b** (88 mg, 0.14 mmol, 86%).

4-[(E)-(2-{1-[2-hydroxy-3-(3-pentadecylphenoxy)propyl]-1H-1,2,3-triazol-4-yl}phenyl)diazenyl]phenol (8a). (10% yield). Orange oil. R_f= 0.31 (hexane/EtOAc, 7.5:2.5); ^{1}H NMR (300.13 MHz, $CDCl_3$) δ 10.34 (s, 1H; OH-Ar), 8.44 (s, 1H; NCH=CNAr), 8.21 (d, ^{3}J(H,H) = 7.89 Hz, 1H; Ar-H), 7.81 (d, ^{3}J(H,H) = 8.77 Hz, 2H; Ar-H), 7.61 (d, ^{3}J(H,H) = 8.19 Hz, 1H; Ar-H), 7.54 (t, ^{3}J(H,H) = 6.80 Hz, 1H; Ar-H), 7.42 (t, ^{3}J(H,H) = 7.60 Hz, 1H; Ar-H), 7.12 (t, ^{3}J(H,H) = 7.16 Hz, 1H; Ar-H), 6.91 (d, ^{3}J(H,H) = 8.84 Hz, 2H; Ar-H), 6,70 (m, 3H; Ar-H), 4.66 (dd, ^{2}J(H,H) = 14.03 Hz, ^{3}J(H,H) = 2.78 Hz, 1H; OCH_2), 4.51 (dd, ^{3}J(H,H) = 6.87 Hz, ^{2}J(H,H) = 14.25 Hz, 1H; OCH_2), 4.21 (m, 1H; CH-OH), 3.91 (m, 2H; CH_2N), 2.46 (m, 25H; CH_2), 1.47 (m, 2H; CH_2), 1.15 (m, 25H; CH_2), 0.78 (m, 3H; CH_3); ^{13}C NMR (75.48 MHz, $CDCl_3$) δ ^{13}C NMR (75.48 MHz, $CDCl_3$) δ 160.80, 158.27, 148.76, 144.75 (4x ArC), 130.27, 129.18, 128.33, 128.11, 127.20, 125.42 (2x), 121.45, 116.20 (2x), 115.74, 114.75, 111.58, 111.46 (2xArC, 1xAr-C=, 1xCH=, 10x ArC-H), 69.15 (O-CH_2), 68.80 (CH-OH), 53.16 (CH_2-N), 35.95 (Ar-CH_2), 33.75, 31.85, 31.35, 29.96, 29.62, 29.46, 29.29, 27.01, 22.62 (CH_2), 19.65 (CH_3); HRMS (ESI) m/z calcd for $C_{38}H_{52}N_5O_3$ 626.4063, found 626.4065.

4-[(E)-(3-{1-[2-hydroxy-3-(3-pentadecylphenoxy)propyl]-1H-1,2,3-triazol-4-yl}phenyl)diazenyl]phenol (8b). (86% yield). Orange solid. Mp: 60-70 ^{o}C. R_f= 0.22 (hexane/EtOAc, 7:3); ^{1}H NMR (300.13 MHz, $CDCl_3$) δ 10.29 (s, 1H; OH-Ar), 8.64 (s, 1H; NCH=CNAr), 8.27 (s, 1H; Ar-H), 7.93 (d, ^{3}J(H,H) = 7.60 Hz, 1H; Ar-H), 7.81 (d, ^{3}J(H,H) = 8.70 Hz, 2H; Ar-H), 7.74 (d, ^{3}J(H,H) = 7.79 Hz, 1H; Ar-H), 7.57 (t, ^{3}J(H,H) = 7.75 Hz, 1H; Ar-H), 7.12 (t, ^{3}J(H,H) = 7.82 Hz, 1H; Ar-H), 6.92 (d, ^{3}J(H,H) = 8.77 Hz, 2H; Ar-H), 6.71 (m, 3H; ArH), 4.63 (dd, ^{2}J(H,H) = 13.66 Hz, ^{3}J(H,H) = 3.65 Hz, 1H; OCH_2), 4.47 (dd, ^{3}J(H,H) = 7.38 Hz, ^{2}J(H,H) = 13.73 Hz, 1H; OCH_2), 4.27 (m, 1H; CH-OH), 3.92 (m, 2H; CH_2N), 2.46 (m, 2H; CH_2), 1.47 (m, 2H; CH_2), 1.15 (m, 25H; CH_2), 0.78 (m, 3H; CH_3); ^{13}C NMR (75.48 MHz, $CDCl_3$) δ 161.59, 158.80, 153.05, 145.95, 145.70, 144.40, 132.48 (6x ArC and 1x Ar-C=), 130.24, 129.58, 127.36, 125.34 (2x), 123.34, 122.11, 121.22, 118.73, 116.36 (2X), 114.98, 112.03 (12x ArC-H and 1x CH=), 69.82 (O-CH_2), 68.31 (CH-OH), 53.43 (CH_2-N), 35.67 (Ar-CH_2), 31.76, 31.33, 29.51, 29.35, 29.18, 22.55 (CH_2), 14.30 (CH_3); HRMS (ESI) m/z calcd for $C_{38}H_{52}N_5O_3$ 626.4066, found 626.4065.

4-[(E)-(4-{1-[2-hydroxy-3-(3-pentadecylphenoxy)propyl]-1H-1,2,3-triazol-4-yl}phenyl)diazenyl]phenol (8c). (62% yield). Orange solid. Mp: 140-145 ^{o}C. R_f= 0.30 (Hexane/EtOAc. 6.5:3.5); ^{1}H NMR (300.13 MHz, $CDCl_3$) δ 10.39 (s, 1H; OH-Ar), 8.67 (s,1H;CH=CNAr), 8.03 (d, ^{3}J(H,H) = 8.50 Hz, 1H; Ar-H), 7.89 (d, ^{3}J(H,H) = 8.50 Hz, 1H; Ar-H), 7.80 (d, ^{3}J(H,H) = 8.85 Hz, 1H; Ar-H), 7.17 (t, ^{3}J(H,H) = 7.50 Hz, 1H; Ar-H), 6.94 (d, ^{3}J(H,H) = 8.85 Hz, 1H; Ar-H), 6.75 (m, 3H; Ar-H), 4.65 (dd, ^{2}J(H,H) = 14.47 Hz, ^{3}J(H,H) = 3.87 Hz, 1H; OCH_2), 4.49 (dd, ^{3}J(H,H) = 7.71 Hz, ^{2}J(H,H) = 13.99 Hz, 1H; OCH_2), 4.27 (m, 1H, CH-OH), 3.95

(m, 2H; CH_2N), 2.50 (m, 2H, CH_2), 1.22 (m, 2H; CH_2), 1.20 (m, 25H, CH_2), 0.83 (m, 3H, CH_3); ^{13}C NMR (75.48 MHz, $CDCl_3$) δ 161.03, 158.37, 151.40, 145.42, 145.37, 144.08, 132.80 (6x ArC and 1x Ar-C=), 129.29, 125.95 (2H), 124.90 (2H), 123.25, 122.90 (2H), 120.94, 116.03 (2H), 114.60, 111.69, (12x ArC-H and 1x CH=), 69.40 (O-CH_2), 67.87 (CH-OH), 53.02 (CH_2-N), 35.23 (Ar-CH_2), 33.72, 31.76, 31.34, 29.07, 28.75, 28.59, 28.48, 22.15 (CH_2), 14.00 (CH_3). ^{13}C NMR (75.48 MHz, $CDCl_3$) δ 160.80, 158.27, 148.76, 144.75 (4x ArC), 130.27, 129.18, 128.33, 128.11, 127.20, 125.42 (2x), 121.45, 116.20 (2x), 115.74, 114.75, 111.58, 111.46 (2xArC, 1xAr-C=, 1xCH=, 10x ArC-H), 69.15 (O-CH_2), 68.80 (CH-OH), 53.16 (CH_2-N),35.95 (Ar-CH_2), 33.75, 31.85, 31.35, 29.96, 29.62, 29.46, 29.29, 27.01, 22.62 (CH_2), 19.65 (CH_3); HRMS (ESI) m/z calcd for $C_{38}H_{52}N_5O_3$ 626.4049, found 626.4065.

Conclusions

We provide an alternative to use cardanol and glycerol as building blocks to produce six amphiphilic molecules. The photophysical results have shown that the synthesized triazolanilines **1a-c** presented good fluorescent features, and are good starting points for research using them as fluorescent markers either on non-polar medium or on targets that require polar specificity. It is worth to point out that **1b** presented a high fluorescent signal at low concentration (4 ppm), and consequently, revealing to be the best candidate to be applied as a marker. Moreover, the blue emission observed for **1c** can be used in applications where an emission in the visible region is desirable. Taking into account that none of the triazoles display fluorescent bands in the region where biodiesel is intrinsic fluorophores as well as fluorescent impurities usually do,[50] compounds **1a-c** ought to be tested as fluorescent markers since they may be an interesting alternative to the conventional ones. On the other hand, azobenzenes **8a-c** have poor fluorescent properties, making them not suitable for use as a fluorescent marker. Finally, all reactions herein reported were carried out under mild conditions and the reagents employed were chosen to minimize the use and generation of hazardous substances.

Acknowledgements

We thank to CNPq for financial support (Grant Numbers: 400119/2014-5 and 404688/2013-6), FUNDECT (PRONEM – Grant Number: 054/12), and Kardol Indústria Química Ltda. Dr Avvari is grateful to Young Talent Fellowship under the Brazilian Scientific Mobility Program "Ciências sem Fronteiras" (Process number: 304629/2014-6). Felipe C. Braga thanks to CAPES for Master Degree scholarship.

Notes and references

1 Moreira LM, dos Santos FB, Lyon JP, Maftoum-Costa M, Pacheco-Soares C, and da Silva NS. Photodynamic Therapy: Porphyrins and Phthalocyanines as Photosensitizers *Aust J Chem* 2008; **61**:741–754.

2 Zhang M, Shu-ting Zheng, Xiao-jing Liu, Ying Long, Bing-qin Yang. A series of novel NIR fluorescent dyes: Synthesis, theoretical calculations and fluorescence imaging applications in living cells. *Dyes Pigm* 2016; **125**:220-228.

3 a) Zhao C, Wang T, Li D, Lu T, Liu D, Meng Q, Zhang Q, Li F, Li W, Hu W, Wang L, Zhou X. Synthesis and characterization of triphenylamine modified azobenzene dyes. *Dyes Pigm* 2017; **137**:256-264. b) Huang Zu-Sheng, Hua T, Tian J, Wang L, Meier H, Cao D. Dithienopyrrolobenzotriazole-based organic dyes with high molar extinction coefficient for efficient dye-sensitized solar cells. *Dyes Pigm* 2016; **125**:229-240.

4 Barona-Castaño JC, Carmona-Vargas CC, Brocksom TJ, de Oliveira KT. Porphyrins as Catalysts in Scalable Organic Reactions. *Molecules* 2016; **21(310)**:1-27

5 a) Linsinger T, Koomen G, Emteborg H, Roebben G, Kramer G, and Lamberty A. Validation of the European Union's Reference Method for the Determination of Solvent Yellow 124 in Gas Oil and Kerosene. *Energy & Fuels* 2004; **18**:1851-1854. b) Krutak JJ, Cushaman MR, Waever MA. US Patent No. 5525516, 1996. c) Friswell MR. US Patent No. 5156653, 1992.

6 Barnsley JE, Shillito GE, Larsen CB, van der Salm H, Wang LE, Lucas NT, and Gordon KC. Benzo[c][1,2,5]thiadiazole Donor−Acceptor Dyes: A Synthetic, Spectroscopic, and Computational Study. *J Phys Chem A* 2016; **120**:1853−1866.

7 Puangmalee S, Petsom A, Thamyongkit P. A porphyrin derivative from cardanol as a diesel fluorescent marker. *Dyes Pigm.* 2009; 82:26-30.

8 Figueira ACB, de Oliveira KT, Serra OA. New porphyrins tailored as biodiesel fluorescent markers. *Dyes Pigm* 2011; **91**:383-388.

9 Tyman JHP. Non-isoprenoid long chain phenols. *Chem Soc Rev* 1979; **8:**522.

10 Rodrigues FHA, França FCF, Souza JRR, Ricardo NMPS and Feitosa JPA. Comparison between physico-chemical properties of the technical Cashew Nut Shell Liquid (CNSL) and those natural extracted from solvent and pressing. *Polímeros* 2011; **21**:156.

11 Setianto WB, Yoshikama S, Smith Jr. RL, Inomata H, Florusse LJ and Peters CJ. Pressure profile separation of phenolic liquid compounds from cashew (Anacardium occidentale)

shell with supercritical carbon dioxide and aspects of its phase equilibria. *J Supercrit Fluids* 2009; **48**:203.

12 Kumar PP, Paramashivappa R, Vithayathil PJ, Rao PVS and Rao AS. Process for Isolation of Cardanol from Technical Cashew (Anacardium occidentale L.) Nut Shell Liquid. *J Agric Food Chem* 2002; **50:**4705.

13 Caló E, Maffezolli A, Mele G, Martina F, Mazetto SE, Tarzia A, Stifani C. Synthesis of a novel cardanol-based benzoxazine monomer and environmentally sustainable production of polymers and bio-composites. *Green Chem* 2007; **9**:754.

14 Attanasi OA, Behalo MS, Favia G, Lomonaco D, Mazzeto SE, Mele G, Piod I, and Vasapollo G. Solvent Free Synthesis of Novel Mono- and Bis-Benzoxazines from Cashew Nut Shell Liquid Components. *Curr Org Chem* 2012; **16**:2613.

15 Mazzetto SE, Lomonaco D, and Mele G. Óleo da castanha de caju: oportunidades e desafios no contexto do desenvolvimento e sustentabilidade industrial. *Quim Nova* 2009; **32**:732.

16 Attanasi OA, Ciccarella G, Filippone P, Mele G, Spadavecchia J, and Vasapollo G. Novel phthalocyanines containing cardanol derivatives. *J Porphyrins Phthalocyanines* 2003; **7:**52.

17 Bloise E, Carbone L, Colafemmina G, D'Accolti L, Mazzetto SE, Vasapollo G, Mele G. First Example of a Lipophilic Porphyrin-Cardanol Hybrid Embedded in a Cardanol-Based Micellar Nanodispersion. *Molecules* 2012; **17**:12252.

18 Mele G, Li J, Margapoti E, Martina F, Vasapollo G. Synthesis of novel porphyrins cardanol based via cross metathesis. *Catalysis Today* 2009; **140**:37.

19 Beatriz A, Araújo YJK and de Lima DP. Glicerol: um breve histórico e aplicação em sínteses estereosseletivas. *Quim. Nova* 2011; **2:**306.

20 Yun D, Kim TY, Park DS, Yun YS, Han JW and Yi J. A Tailored Catalyst for the Sustainable Conversion of Glycerol to Acrolein: Mechanistic Aspect of Sequential Dehydration. *ChemSusChem* 2014; **7**:2193.

21 Ruppert AM, Weinberg K and Palkovits R. Hydrogenolysis Goes Bio: From Carbohydrates and Sugar Alcohols to Platform Chemicals. *Angew Chem Int Ed* 2012; **51**:2564.

22 Sonnati MO, Amigoni S, Givenchy EPT, Darmanin T, Choulet O and Guittard F. Glycerol carbonate as a versatile building block for tomorrow: synthesis, reactivity, properties and applications. *Green Chem* 2013; **15**:283.

23 Calvino-Casilda V, Guerrero-Pérez MO and Bañares MA. Microwave-activated direct synthesis of acrylonitrile from glycerol under mild conditions: Effect of niobium as dopant of the V-Sb oxide catalytic system. *Appl Catal* B 2010; **95**:192.

24 Chheda JN, Huber GW and Dumesic JA. Liquid-Phase Catalytic Processing of Biomass-Derived Oxygenated Hydrocarbons to Fuels and Chemicals. *Angew Chem Int E* 2007; **46**:7164.

25 Hou J, Liu X, Shen J, Zhao G and Wang PG. The impact of click chemistry in medicinal chemistry. *Expert Opin Drug Discov* 2012; **7**:489.

26 Ghosh D, Rhodes S, Hawkins K, Winder D, Atkinson A, Ming W, Padgett C, Orvis J, Aiken K and Landge S. A simple and effective 1,2,3-triazole based "turn-on" fluorescence sensor for the detection of anions. *New J Chem* 2015; **39**:295.

27 Kolb HC, Finn MG and Sharpless KB. Click Chemistry: Diverse Chemical Function from a Few Good Reactions. *Angew Chem Int Ed* 2001; **40**:2004-2021.

28 Sergeevich GD and Nikolaevich LZ. Hydrochlorination of Glycerol - The Role of the Water on the Process. *J Chem Chem Eng* 2011; **5**:1179-1182.

29 Das B, Reddy VS, Tehseen F and Krishnaiah M. Catalyst-Free Highly Regio- and Stereoselective Ring Opening of Epoxides and Aziridines with Sodium Azide Using Poly(ethylene glycol) as an Efficient Reaction Medium. *Synthesis* 2007; 666-668.

30 Maryamabadi A, Hasaninejad A, Nowrouzi N, Mohebbi G and Asghari B. Application of PEG-400 as a green biodegradable polymeric medium for the catalyst-free synthesis of spiro-dihydropyridines and their use as acetyl and butyrylcholinesterase inhibitors. *Bioorg Med Chem* 2016; **24**:1408-1417.

31 Chandrasekhar S, Narsihmulu C, Sultana SS and Reddy NRK. Poly(ethylene glycol) (PEG) as a Reusable Solvent Medium for Organic Synthesis. Application in the Heck Reaction. *Org Lett* 2002; **4**:4399-4401.

32 Namboodiri VV and Varma RS. Microwave-accelerated Suzuki cross-coupling reaction in polyethylene glycol (PEG). *Green Chem* 2001; **3**:146-148.

33 Yedage SL and Bhanage BM. Ru(II)/PEG-400 as a highly efficient and recyclable catalytic media for annulation and olefination reactions via C–H bond activation. *Green Chem* 2016; 18:5635-5642. DOI: 10.1039/c6gc01581f

34 Nakanishi K and Solomon PH, *Infrared Absorption Spectroscopy* 2nd ed., Holding-Day, 1977.

35 Rostovtsev VV, Green LG, Fokin VV, Sharpless KB. Microwave-accelerated Suzuki cross-coupling reaction in polyethylene glycol (PEG). *Angew Chem* 2002; **41**:2596-2599.

36 Prasad AN, Thirupathi B, Raju G, Srinivas R and Reddy BM. One pot 'click' reaction: CuII–hydrotalcite catalyzed tandem synthesis of β-hydroxy triazoles via regioselective opening of epoxide followed by [3+2] cycloaddition. *Catal Sci Technol* 2012; **2**:1264-1268.

37 a) Wakatsuki Y, Yamazaki H, Grutsch PA, Santhanam M, Kutal C. Study of intramolecular sensitization and other excited-state pathways in orthometalated azobenzene complexes of palladium(II). *J Am Chem Soc* 1985, **107**:8153-8159; b) Shimomura M, Kunitake T. Fluorescence and photoisomerization of azobenzene-containing bilayer membranes. *J Am Chem Soc* 1987; **109**:5175-5183; c) Ghedini M, Pucci D, Calogero G, Barigelletti F. Luminescence of azobenzene derivatives induced by cyclopalladation *Chem Phys Lett* 1997, **267**:341-344; d) Ghedini M, Pucci D, Crispini A, Aiello I, Barigelletti F, Gessi A and Francescangeli O. Dinuclear cyclopalladated azobenzene complexes: a comparative study on model compounds for organometallic liquid-crystalline materials. *Appl Organomet Chem* 1999; **13**; 565-581; e) Aiello I, Ghedini M and La Deda M. Synthesis and spectroscopic characterization of organometallic chromophores for photoluminescent materials: cyclopalladated complexes. *J Lumin* 2002; **96**:249-259; f) Han M and Hara M. Intense Fluorescence from Light-Driven Self-Assembled Aggregates of Nonionic Azobenzene Derivative. *J Am Chem Soc* 2005; **127**:10951-10955; g) Han MR and Hara M. Chain length-dependent photoinduced formation of azobenzene aggregates. *New J Chem* 2006; **30**:223-227; h) Ran X, Wang H, Shi L, Lou J, Liu B, Li M, Guo L. Light-driven fluorescence enhancement and self-assembled structural evolution of an azobenzene derivative. *J Mater Chem C* 2014; **2**:9866-9873.

38 Yoshino J, Kano N, Kawashima T. Fluorescent azobenzenes and aromatic aldimines featuring an N–B interaction. *Dalton Trans* 2013; **42**:15826-15834.

39 a) Rau H and Lueddecke E. On the rotation-inversion controversy on photoisomerization of azobenzenes. Experimental proof of inversion. *J Am Chem Soc* 1982; **104**:1616-1620; b) Ingale G and Seo YJ. Azo compounds with different sized fluorophores and characterization of their photophysical properties based on trans to cis conformational change. *Tetrahedron Lett* 2014; **55**:5247-5250.

40 Dewar MJS, Zoebisch EG, Healy EF and Stewart JPJ. Development and use of quantum mechanical molecular models. 76. AM1: a new general purpose quantum mechanical molecular model. *J Am Chem Soc* 1985; **107**:3902-3909.

41 Fabian WMF. Substituent effects on absorption and fluorescence spectra of carbostyrils. *J Mol Struct* 1999; **477**:209-220.

42 Zerner MC, Reidlinger C, Fabian WMF and Junek H. Push–pull dyes containing malononitrile dimer as acceptor: synthesis, spectroscopy and quantum chemical calculations. *J Mol Struct (THEOCHEM)* 2001; **543**:129-146.

43 Kimura K, Tsubomura H and Nagakura S. The Vacuum Ultraviolet Absorption Spectra of Aniline and Some of Its N-Derivatives. *Bull Chem Soc Jpn* 1964; **37**:1336-1346.

44 Cogan S, Zilberg S and Haas Y. The Electronic Origin of the Dual Fluorescence in Donor−Acceptor Substituted Benzene Derivatives. *J Am Chem Soc* 2006; **128**; 3335-3345.

45 Crivelaro F, Oliveira MRS, Lima SM, Andrade LHC, Casagrande GA, Raminelli C and Caires ARL. Fluorescence analysis of iodinated acetophenone derivatives. *Spectrochimica Acta Part A: Molecular and Biomolecular Spectroscopy* 2015; **139**:63-67.

46 Smith MJ. US patent no. 5498808. Chem abstr 1996; Chem Abstr. 1996, 124, 294047.

47 Hamon F, Djedaini-Pilard F, Barbot F and Len C. Azobenzenes - synthesis and carbohydrate applications. *Tetrahedron* 2009; **65**:10105-10123.

48 Jung JH, Lee SJ, Kim JS, Lee WS, Sakata Y and Kaneda T. α-CD/Crown-Appended Diazophenol for Selective Sensing of Amines. *Org Lett* 2006; **8**:3009-3012.

49 Valeur B, Molecular Fluorescence: Principles and Applications, Wiley-VCH, New York, 2001. DOI: https://doi.org/10.1002/3527600248

50 Magalhães KF, Caires ARL, Silva MS, Alcantara GB, Oliveira SL. Endogenous fluorescence of biodiesel and products thereof: Investigation of the molecules responsible for this effect. *Fuel* 2014; **119**:120–128

Legendo of Tables

Table 1 Optimization studies for ring opening of epoxide with azide.[a]

Table 2 Optimization reaction conditions for 1,2,3-triazoles.[a]

Table 3 Main electronic transition determined by AM1 semi-empirical method (in vacuum). Details can be accessed in Table S1 in the Supplementary materials.

Table 4 Fluorescence quantum yield obtained by calculating the absorption and fluorescence intensities.

Table 5 Main electronic transition determined by AM1 semi-empirical method (in vacuum). For the complete results see Table S2 in the Supplementary materials.

Tables

Table 1

Entry	Solvent	Temp (^{0}C)	Yield (%)
1	DMF	140	45
2	DMF	r.t.	-
3	THF	r.t.	20
4	MeOH	r.t.	15
5	PEG 200	r.t.	57
6	PEG 400	60	87
7	Solvent-free	r.t.	-
8	CH_3CN	r.t.	18

[a]Reaction conditions: Epoxide **5a** (0.14 mmol), sodium azide (0.21 mmol) and PEG-400 (1.5 mL) stirred for about 4 h.

Table 2

Entry	Catalyst	Solvent	Temp (^{0}C)	Yield (%)
1	CuCl	CH_3CN	r.t.	-
2	CuBr	CH_3CN	r.t.	10
3	$Cu(OAc)_2$	H_2O	r.t.	-
4	$Cu(OAc)_2$	MeOH	r.t.	15
5	Cu (0) powder	H_2O/^{t}BuOH (2:1)	r.t.	34
6	Cu (0) powder	DMF	140	12
7	CuCl	THF	80	-
8	$Cu(OAc)_2$	EtOH	60	18
9	Cu (0) powder	H_2O/Acetone (2:1)	r.t.	69
10	-	H_2O/Acetone (2:1)	25-80	-
11	Cu (0) powder	Solvent-free	r.t.	42
12	$CuSO_4.5H_2O$/NaASc	H_2O/Acetone (2:1)	r.t	28

[a]Reaction conditions: Compound **7** (0.078 mmol), terminal alkyne **6c** (0.11 mmol), catalyst (10 mg) and solvent (2 mL) stirred for about 12 h.

Table 3

Absorption range	1a		1b		1c	
	λ (nm)	Oscillator trength	λ (nm)	Oscillator strength	λ (nm)	Oscillator strength
a	204	0.36	207	0.59	205	0.45
	216	1.11	220	0.66	-	-
b	226	0.31	224; 226	0.10; 0.14	225	0.24
	259	0.33	258	0.57	-	-
c	278	0.20	274	0.20	-	-
	-	-	-	-	284	0.35

Table 4

Sample ratio	Φ_F ratio
1b /1a	9.35
1b /1c	6.32
1c /1a	1.74

Table 5

Absorption range	8a		8b		8c	
	Wavenumber (nm)	**Oscillator strength**	**Wavenumber (nm)**	**Oscillator strength**	**Wavenumber (nm)**	**Oscillator strength**
a	216	0.21				
			235	0.35	231	0.42
	238	0.94	241	0.52	241	0.24
b	242	0.28	248	0.28	264	0.02
	250	0.44	258	0.40	270	0.12
	261	0.21	265	0.24		
	270	0.07				
	288	0.21				
c	324	0.62	296	0.09	353	1.48
			325	1.17		

Legends of Figures

Figure 1 Chemical structures of CNSL´s main components.

Figure 2 General structure of the target compounds.

Figure 3 Absorption spectra of 1a-c when diluted in CH_2Cl_2 at 4 ppm. The letters represent the electronic bands obtained by AM1 semi-empirical method as presented in details in Table 3.

Figure 4 Fluorescence spectra of **1a-c** when excited at 265 nm and diluted in CH_2Cl_2 at 4 ppm. Inset: Normalized Fluorescence spectra.

Figure 5 Excitation-Emission map of **1a-c** when diluted in CH_2Cl_2 at 4 ppm.

Figure 6 Absorption spectra of **8a-c** when diluted in CH_2Cl_2 at 4 ppm. The letters represent the electronic bands obtained by AM1 semi-empirical method as presented in details in Table 5.

Figures

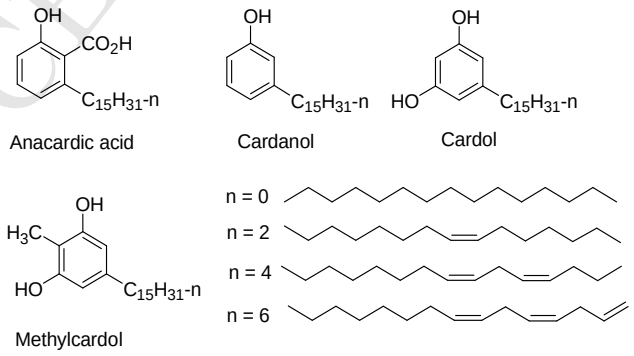

Figure 1

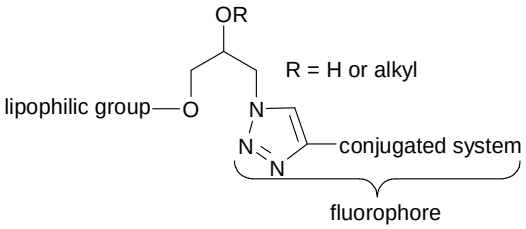

Figure 2

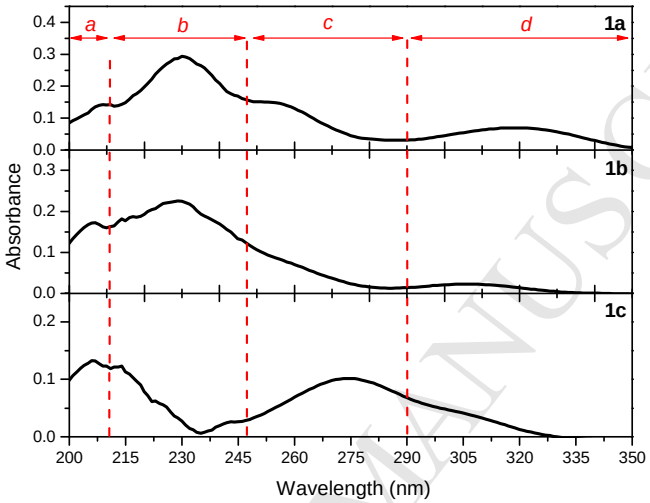

Figure 3

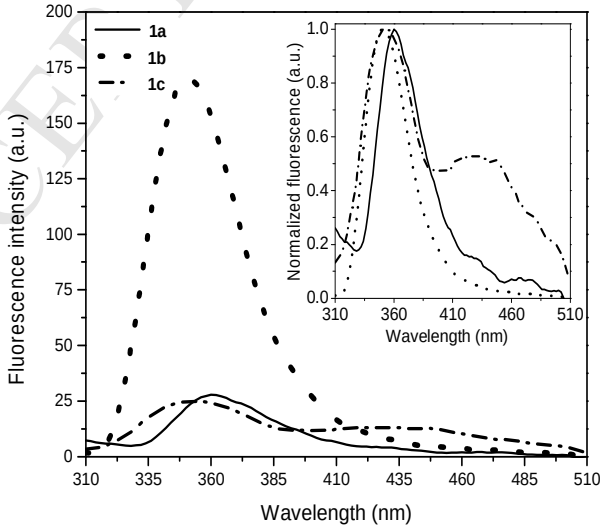

Figure 4

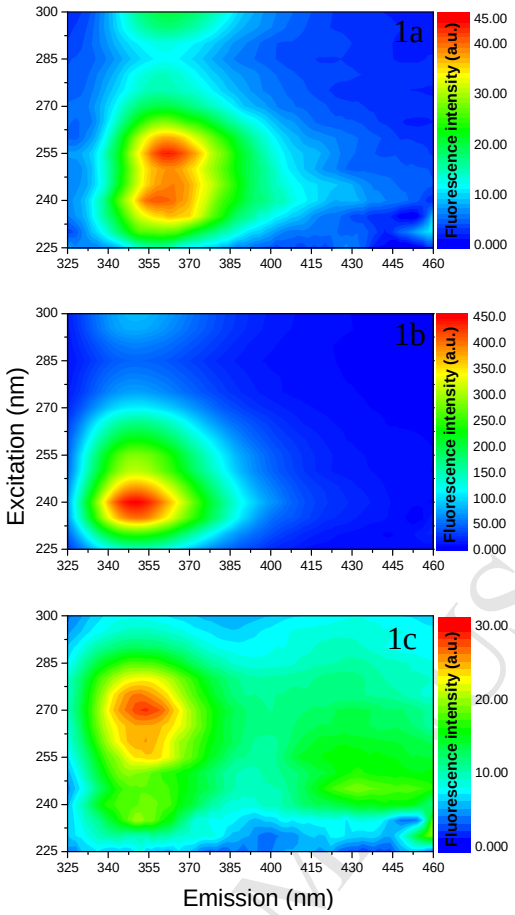

Figure 5

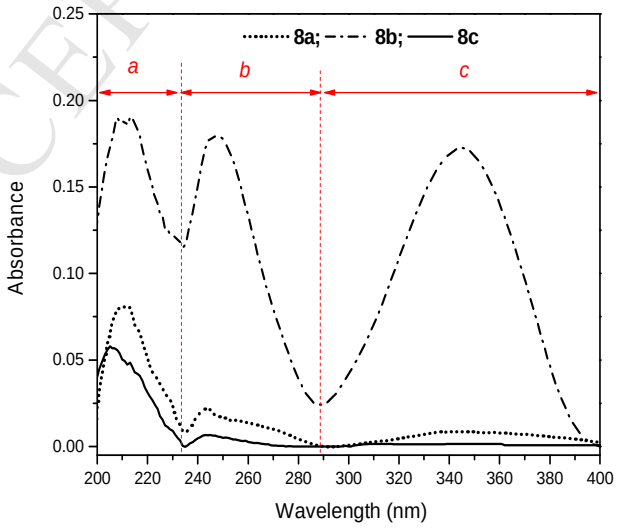

Figure 6

Legends of schemes

Scheme 1 Retrosynthetic analysis to achieve potential fluorescent products.

Scheme 2 Reaction of cardanol with epichlorohydrin.

Scheme 3 Synthetic route for triazolanilines **8a-c**.

Scheme 4 Synthesis of azobenzenes **8a-c**.

Schemes

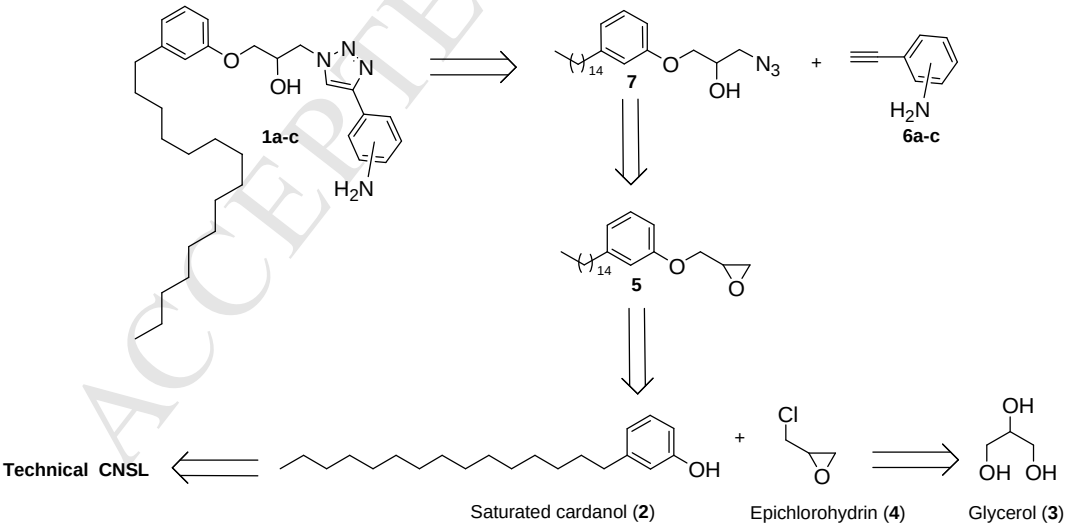

Scheme 1

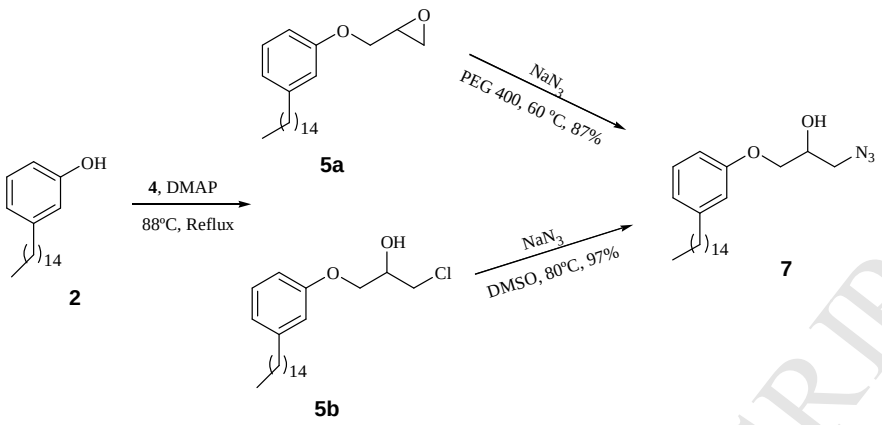

Scheme 2

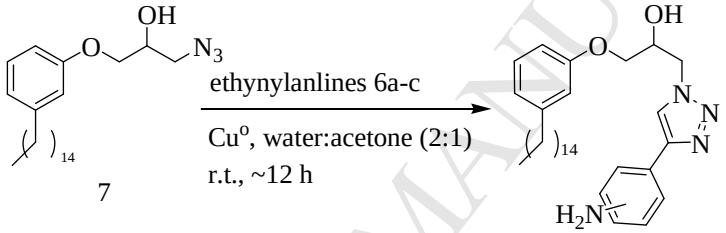

1a = 2-NH_2 (54%)
1b = 3-NH_2 (83%)
1c = 4-NH_2 (96%)

Scheme 3

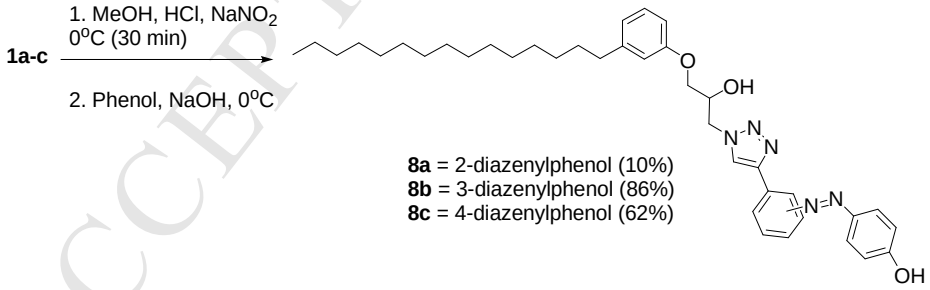

8a = 2-diazenylphenol (10%)
8b = 3-diazenylphenol (86%)
8c = 4-diazenylphenol (62%)

Scheme 4

HIGHLIGHTS

We provide an alternative to use cardanol and glycerol as building blocks to produce novel fluorescent 1,4-disubstituted-1,2,3-triazoles. The *meta*-triazolaniline presented a high fluorescent signal at low concentration.